Time to failure prediction in rubber components subjected to thermal ageing: A combined approach based upon the intrinsic defect concept and the fracture mechanics

M. Ben Hassine [a,b], M. Naït-Abdelaziz [c,*], F. Zaïri [c], X. Colin [a], C. Tourcher [b], G. Marque [b]

[a] *Laboratoire des Procédés et Ingénierie en Mécanique et Matériaux (PIMM), UMR CNRS 8006, Arts et Métiers ParisTech, 151 boulevard de l'Hôpital, F-75013 Paris, France*
[b] *EDF R&D, avenue des Renardières, F-77818 Moret-sur-Loing, France*
[c] *Laboratoire de Mécanique de Lille (LML), UMR CNRS 8107, Université Lille 1 Sciences et Technologies, avenue Paul Langevin, F-59650 Villeneuve d'Ascq, France*

Keywords:
Rubber
Thermal ageing
Failure prediction
Intrinsic defect
Fracture mechanics

A B S T R A C T

In this contribution, we attempt to derive a tool allowing the prediction of the stretch ratio at failure in rubber components subjected to thermal ageing. To achieve this goal, the main idea is to combine the fracture mechanics approach and the intrinsic defect concept. Using an accelerated ageing procedure for an Ethylene–Propylene–Diene Monomer (EPDM), it is first shown that the average molar mass of the elastically active chains (i.e. between cross-links) can be used as the main indicator of the macromolecular network degradation. By introducing the time–temperature equivalence principle, a shift factor obeying to an Arrhenius law is derived, and master curves are built as well for the average molar mass as for the ultimate mechanical properties. Fracture mechanics tests are also achieved and the square root dependence of the fracture energy with the average molar mass is pointed out. Moreover, it is shown that the mechanical response could be approximated by the phantom network theory, which allows to relate the strain energy density function to the average molar mass. Assuming that the fracture of a smooth specimen is the consequence of a virtual intrinsic defect whose the size can be easily estimated, the stretch ratio at break can be therefore computed for any thermal ageing condition. The estimated values are found in a very nice agreement with EPDM experimental data, making this approach a useful tool when designing rubber components for moderate to high temperature environments.

1. Introduction

The use of rubber components is very widespread in many industrial domains as, for example, in ground or air transportation, medical equipment, electrical insulation, mechanical damping, etc. They can consequently be subjected to complex mechanical loadings in various environmental conditions. Because of the dependence of the mechanical properties either on the kind of loading or on the operating environment (light, humidity, temperature, oxygen, etc.), an optimal design of these components must account for the alteration of the mechanical properties due to ageing. Indeed, chemical and physical ageings are known to strongly modify the mechanical responses of such materials, but also the ultimate properties. Especially, in the presence of oxygen, the modification of the chemical structure of the elastomeric material is essentially attributed to the macromolecular chain scissions and

* Corresponding author.
E-mail address: moussa.nait-abdelaziz@univ-lille1.fr (M. Naït-Abdelaziz).

crosslinking in addition to the break and reformation of crosslink nodes (Rajeev et al., 2003; Rivaton et al., 2005; Colin et al., 2007a; Tomer et al., 2007). These mechanisms induce the alteration of the mechanical properties (Clavreul, 1997; Assink et al., 2002; Colin et al., 2007a).

Chemical ageing of polymers is generally investigated by using analytical techniques allowing the measurement of their chemical, physical and mechanical properties (Colin et al., 2007a,b,c). Since ageing is a long time process, accelerated thermal ageing tests are often used to shorten their exposure duration and predict their operating life time. In fact, from these tests, results for lower temperatures are generally obtained using the time–temperature equivalence principle (Ferry, 1970; Treloar, 1971; Ha-Anh and Vu-Khanh, 2005; Gillen et al., 2006; Woo and Park, 2011).

The purpose of this contribution is the prediction of stretch ratio at failure in rubbers subjected to thermal ageing conditions. To achieve this goal, the main idea is to combine the fracture mechanics approach and the intrinsic defect concept. This combined approach[1] was successfully introduced to study the biaxial fracture of rubbers (Naït-Abdelaziz et al., 2012) and is extended here in order to propose a failure criterion accounting for degradation due to thermal ageing.

This paper is organised as follows. In Section 2, a general background on the main tools involved in this paper is presented. It mainly includes fracture mechanics of rubbers, large strain elastic constitutive models and time–temperature equivalence. Material and experimental procedure are detailed in Section 3. In Section 4, experimental results are reported. The predictive approach is presented in Section 5: estimations are compared to experimental data. Concluding remarks close the paper in Section 6.

2. A brief literature background

2.1. Fracture mechanics of rubbers

Since the pioneering work of Griffith (1921), fracture mechanics can generally be tackled via an energy balance which defines a parameter called the strain energy release rate G defined such as:

$$G = -\frac{\partial U}{\partial A} \tag{1}$$

where U is the potential energy and A is the crack area. At crack initiation, the strain energy release rate G takes a critical value generally called the fracture energy and noted G_c which is considered as an intrinsic material property. Based upon this definition, Rivlin and Thomas (1953) introduced the tearing energy T_c, equivalent to G_c, in the case of elastomers. From a simple analysis of the modification in the stored energy in a specimen containing an edge crack of length a, they expressed T_c in the following form:

$$T_c = G_c = 2k(\lambda_c)W_c a \tag{2}$$

where W_c is the critical strain energy density and k is a factor depending on the stretch ratio $\lambda = l/l_0$. The suffix c denotes the critical value corresponding to crack initiation.

The k factor depends on the specimen geometry. As an example, according to Greensmith (1963) in the case of Single Edge Notched Tension (SENT) specimens, this parameter is expressed as follows:

$$k(\lambda) = \frac{2.95 - 0.08(1-\lambda)}{\sqrt{\lambda}} \tag{3}$$

This result, based upon experimental data, was confirmed by a finite element (FE) analysis by Lindley (1972). Let us note that the energy interpretation of the J integral introduced by Rice (1968) and Cherepanov (1968) is equivalent to the strain energy release rate G for elastic materials. Thus, the fracture energy can be also evaluated by using the J integral. The fracture mechanics properties are dependent on the sharpness of the notch (Trapper and Volokh, 2008; Volokh, 2013) and this influence decreases when large strain is involved since the crack radius increases to form a smooth notch (Naït-Abdelaziz et al., 2012).

Dealing with multiaxial fracture of rubbers, in the case of circular defects, Naït-Abdelaziz et al. (2012) have proposed a general form for T which accounts for the biaxiality ratio at large strain:

$$T = G = J = 2\lambda_{eq}^{\gamma} g(\lambda_{eq}) W a \tag{4}$$

in which γ is a parameter depending on the biaxiality ratio ranging approximately from 1 (uniaxial tension) to 1.4 (equibiaxial tension) and λ_{eq} is the equivalent stretch ratio expressed as a function of the principal stretches:

$$\lambda_{eq} = \sqrt{\frac{\lambda_1^2 + \lambda_2^2 + \lambda_3^2}{3}} \tag{5}$$

in which λ_1, λ_2 and λ_3 are the principal stretches.

The function g in Eq. (4) depends on the equivalent stretch ratio and can be fitted by the following equation:

$$g(\lambda_{eq}) = 0.255 + \frac{2.837}{(\lambda_{eq})^2} - \frac{2.888}{(\lambda_{eq})^4} + \frac{2.507}{(\lambda_{eq})^6} \tag{6}$$

2.2. Constitutive mechanical models

The basic features of the rubber stress–strain response are generally described by large strain elastic constitutive models which can be classified into two categories: the first one, physically-based, is issued from statistical mechanics theories (Treloar, 1943; James and Guth, 1943; Arruda and Boyce, 1993) and the second one, phenomenological-based, is issued from invariant-based and stretch-based continuum mechanics approaches (Rivlin, 1948; Ogden, 1984; Yeoh, 1990). The invariant-based Rivlin (1948) and stretch-based Ogden (1984) phenomenological models are probably the most popular and are expressed in terms of strain energy density (SED) functions, respectively, as follows:

[1] It is based upon the assumption that defects always exist in a given material and act as stress concentrators. Consequently, the material failure is the consequence of the growth of virtual cracks.

$$W = \sum_{i=0}^{\infty}\sum_{j=0}^{\infty} C_{ij}(I_1 - 3)^i (I_2 - 3)^j \tag{7}$$

$$W = \sum_{i=1}^{\infty} \frac{\mu_i}{\alpha_i}(\lambda_1^{\alpha_i} + \lambda_2^{\alpha_i} + \lambda_3^{\alpha_i} - 3) \tag{8}$$

where I_1 and I_2 are the two first invariants of the right Cauchy–Green strain tensor. The terms C_{ij}, α_i and μ_i are material parameters to be identified experimentally.

Let us now highlight the particular case of a first-order development in the invariant-based Rivlin (1948) model (i.e. $j = 0$ and $i = 1$). In this case, the SED function given in Eq. (7) reduces to:

$$W = C_{10}(I_1 - 3) = C_{10}(\lambda_1^2 + \lambda_2^2 + \lambda_3^2 - 3) \tag{9}$$

Note that a first-order development of the stretch-based Ogden (1984) model given in Eq. (8) leads to:

$$W = \frac{\mu_1}{\alpha_1}(\lambda_1^{\alpha_1} + \lambda_2^{\alpha_1} + \lambda_3^{\alpha_1} - 3) \tag{10}$$

which reveals that Eqs. (9) and (10) are formally equivalent if $\alpha_1 = 2$ and $C_{10} = \mu_1/2$. For this particular case, the parameter μ_1 is the so-called shear modulus.

A physically-based approach (Treloar, 1943), describing the kinematics of a single macromolecular chain in the framework of the statistical mechanics allowed to get, for a perfect network, the so-called Neo-hookean model. In this statistical Gaussian model which represents the fundament of the rubber elasticity, the SED function is expressed as follows:

$$W = \frac{nkT}{2}(\lambda_1^2 + \lambda_2^2 + \lambda_3^2 - 3) \tag{11}$$

where n is the density of the elastically active chains, k is the Boltzmann constant and T is the absolute temperature which underlines the entropic nature of the rubber elasticity. Comparing Eqs. (9)–(11) it comes that:

$$\mu_1 = 2C_{10} = nkT \tag{12}$$

The previous model assumes a perfect network (also called affine network). Particularly, in this approach, the terminations of the network elastic segments are supposed to be fixed. In a real network, these terminations play the role of junction nodes of different elastic segments (crosslinking nodes for example) and can therefore move around a mean position. To account for the mobility of these junction nodes, James and Guth (1943) modified the Neo-hookean model and derived the so-called phantom network model expressed as follows:

$$W = \frac{nkT}{2}\left(1 - \frac{2}{f}\right)(\lambda_1^2 + \lambda_2^2 + \lambda_3^2 - 3) \tag{13}$$

In Eq. (13), f is the crosslink functionality (i.e. the number of the elastically active chains linked to the same crosslink node) whose a common value is 3 or 4 for rubbers.

It can be alternatively written as follows:

$$W = \frac{\rho RT}{2M_c}\left(1 - \frac{2}{f}\right)(\lambda_1^2 + \lambda_2^2 + \lambda_3^2 - 3) \tag{14}$$

and, when considering uniaxial tension:

$$W = \frac{\rho RT}{2M_c}\left(1 - \frac{2}{f}\right)\left(\lambda^2 + \frac{2}{\lambda} - 3\right) \tag{15}$$

where R is the perfect gas constant, ρ is the reference mass density for a given state of ageing and M_c is the average molar mass of the elastically active chains (i.e. between crosslinks).

2.3. Intrinsic defect concept

Perfect materials do not exist in nature, and all materials generally contain flaws issued from processing or preageing (such as voids and micro-cracks). Rubbers are generally reinforced by particles and mainly by carbon black. This filler is generally very small (its size is lower than 100 nm). Nevertheless, it can form aggregates of which the size can reach a few microns. These aggregates can play a role of intrinsic defects which act as potential cracks. They directly affect the strength (Bueche, 1959; Roland and Smith, 1985) or the fatigue life properties (Braden and Gent, 1960; Gent et al., 1964; Choi and Roland, 1996).

The approach we have developed in Naït-Abdelaziz et al. (2012) is founded on the assumption that the failure of a smooth specimen loaded in tension could be attributed to the propagation of the intrinsic defect. So, for a given defect size, if the fracture toughness in terms of J_c is available, then we can derive the stretch ratio at failure from Eq. (4). In this study, the intrinsic defect was calculated by using Eq. (4), the inputs being the fracture energy J_c, the stretch ratio at break of a smooth specimen in tension λ_c and the SED function W. From this approach, we have estimated the stretch ratios at break for different loading paths (i.e. biaxiality ratios) and found a very nice agreement with experimental data for a Natural Rubber and a Styrene Butadiene Rubber.

The objective of this contribution is to estimate the stretch ratios at break under tension loading for various thermal ageing conditions. The adopted approach is to calculate the intrinsic defect for a virgin (unaged) material and to derive the stretch ratios for the thermally aged materials, the J_c value and also the SED function being available for each time of exposure. This methodology will be detailed further.

2.4. Time–temperature equivalence

The time–temperature principle was specifically investigated to address the issue of the similarity in the evolution of the mechanical behaviour of viscoelastic materials (such as polymers) when increasing the strain rate or decreasing the temperature (Treloar, 1971). It consists in constructing a so-called master curve from the measurements of a mechanical property (modulus for example) in a given range of temperatures (or strain rates) for different strain rates (or temperatures). The obtained curves can be then superimposed by shifting them via a shift factor noted a_T to get the master curve for the mechanical property under investigation. Therefore, this master curve allows to estimate the mechanical property for a

temperature or a strain rate value (not experimentally measurable) by extrapolation. The shift factor can be fitted using an Arrhenius type law which takes the following form:

$$\ln(a_T) = -\frac{E_a}{R}\left(\frac{1}{T} - \frac{1}{T_0}\right) \tag{16}$$

where E_a is the activation energy, T is the absolute temperature, T_0 is the reference temperature and R is the perfect gas constant.

This form is generally used when $T_0 > T_g + 100$, T_g being the glass transition temperature of the polymer. This model has been widely and successfully used to investigate the thermal ageing of polymers (Ha-Anh and Vu-Khanh, 2005; Gillen et al., 2006; Woo and Park, 2011). When the previous restriction on the reference temperature is no longer valid, one may use the phenomenological approach developed by Williams–Landel–Ferry (Williams et al., 1955), known as the WLF approach. According to these authors, the shift factor can be approximated by the following expression:

$$\ln(a_T) = \frac{C_1(T - T_0)}{C_2 + T - T_0} \tag{17}$$

in which C_1 and C_2 are two adjustable parameters depending on the material under study.

3. Material and experimental procedure

3.1. Material

The material investigated in this work is an Ethylene–Propylene–Diene Monomer (EPDM) rubber. It consists in the following molar fractions of monomer units: 66.1 mol.% ethylene, 33.1 mol.% propylene and 0.8 mol.% norbornene (ENB). It is vulcanised by 4 phr of sulphur compounds and filled by 13 and 29.8 wt% of carbon black and clay platelets, respectively.

3.2. Specimens

Three specimen kinds were used in this work. They were cut from EPDM sheets. The average molar mass measurements were achieved using circular flat discs. Dogbone specimens were selected to achieve tensile tests and get the stress–strain relationship and the ultimate properties. Double Edge Notched Tension (DENT) specimens were chosen to measure the fracture energy. Note that the thickness of these three specimen kinds is the same and equal to 3.8 mm. Fig. 1 shows the specimen geometries.

3.3. Accelerated ageing procedure

The three specimen kinds were exposed in air-ventilated ovens at 130, 150 and 170 °C for various exposure times. Let us note that a dedicated set-up was designed in order to keep the dogbone and DENT specimens in a vertical position and thus, avoid any change in form during their exposure to high temperature in the air-ventilated ovens.

3.4. Average molar mass measurements

For each test condition in terms of ageing temperature and exposure time, the average molar mass of the elastically active chains M_c was determined by swelling in cyclohexane at 25 °C in a Soxhlet apparatus. Indeed, when a rubbery polymer network is placed in a suitable solvent (presenting a good chemical affinity with the polymer), the polymer tends to absorb the maximum of solvent in its free volume (Fig. 2a). This reversible physical process causes the network volume expansion in the three space directions as shown in Fig. 2b.

This swelling ability depends on the interactions between the polymer chains and solvent molecules, in addition to the length of polymer chains between cross-links which is defined by the average molar mass of the elastically active chains M_c. This parameter is given by the Flory–Rehner relationship for a 4-functional network (Marzocca, 2007):

$$M_c = -\frac{0.5V\rho_{polymer}(V_{r0}^{1/3} - 0.5V_{r0})}{\ln(1 - V_{r0}) + V_{r0} + \chi V_{r0}^2} \tag{18}$$

where V is the molar volume of the solvent (cm^3/mol), $\rho_{polymer}$ is the polymer density (0.86 g/cm^3 for EPDM), χ is the Flory–Huggins interaction parameter between the polymer and the solvent equal to 0.321 for EPDM-cyclohexane (Baldwin and Ver Strate, 1972; Hilborn and Ranaby, 1989) and V_{r0} is the polymer volume fraction in the swollen network expressed as:

$$V_{r0} = \frac{\rho_{solvent}}{\rho_{solvent} + (m_g/m_s - 1)\rho_{polymer}} \tag{19}$$

where m_g is the weight of swollen polymer sample, m_s is the weight of the same sample after drying under vacuum at 40 °C for 24 h and $\rho_{solvent}$ is the solvent density (0.78 g/cm^3 for cyclohexane).

3.5. Tensile and fracture mechanics tests

Monotonic tensile tests were performed in order to get the stress–strain relationship and the ultimate properties (in terms of strain and stress at break). Tests were achieved until fracture at room temperature (25 °C) and under a constant crosshead speed of 5 mm/mn on an electromechanical Instron 5800 set-up equipped with a load cell of 1 kN. Strains were measured using a non-contact video-system allowing to track the displacement of two spots previously printed on the dogbone specimens. For each exposure time and temperature, seven tests were carried out to estimate the natural scattering of the mechanical response.

Fracture tests were achieved in order to estimate the fracture toughness in terms of fracture energy G_c by using the DENT specimens. They were performed with the same apparatus used for the tensile tests at room temperature and under a constant crosshead speed of 15 mm/min.

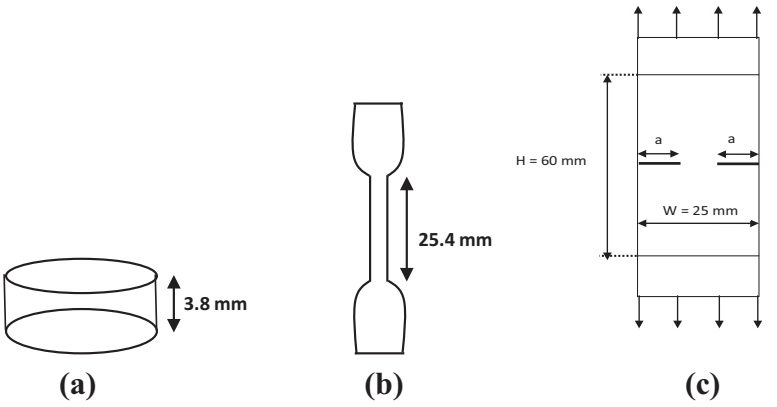

Fig. 1. Specimen geometries for: (a) average molar mass measurements, (b) tensile and (c) fracture mechanics tests.

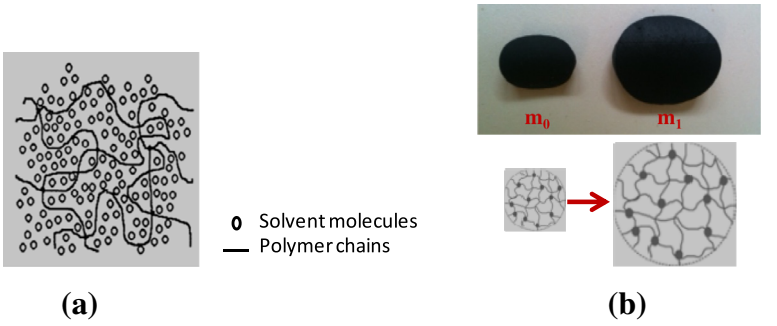

Fig. 2. Polymer network swollen in an adequate solvent (a) and EPDM swelling in the cyclohexane solvent (b).

4. Experimental results

4.1. Average molar mass

The average molar mass dependence on both temperature and exposure time is shown in Fig. 3a. As expected, increasing the exposure time leads to the decrease of the average molar mass while increasing the temperature accelerates this process. Using Eq. (16), the time–temperature equivalence was applied to the average molar mass data. The best shift factor, for a reference temperature of 403 K, was obtained by using an activation energy equal to 104 kJ/mol. This value is in the same order of magnitude than that given by Ajalesh Balachandran et al. (2012). It appears that the average molar mass could be taken as a parameter reflecting the degradation state of the material. The evolution of the average molar mass as a function of the reduced time ta_T, shown in Fig. 3b, can be fitted by a decreasing exponential law of the form:

$$M_c = \beta + \delta e^{-\eta t a_T} \tag{20}$$

where β, δ and η are constants determined using a least square method which values are $\beta = 600$ g/mol, $\delta = 1100$ g/mol and $\eta = 9.5 \cdot 10^{-4}$ h^{-1}.

4.2. Ultimate properties

From the uniaxial tensile tests, failure strain and stress were measured for each ageing condition (temperature and exposure time). As expected, either the failure strain or the failure stress decreases when increasing the exposure time at a given temperature. This decrease is dramatically amplified when increasing the temperature. Fig. 4 shows the changes in these ultimate properties as a function of the reduced time, after applying the time–temperature equivalence principle. Note that the same value of the activation energy as that calculated for the average molar mass was used to shift these data. That is to say that the same value of the shift factor was used in this case. In Fig. 4a is shown the evolution of the failure stretch ratio while in Fig. 4b the true stress at break is reported. As clearly shown in these figures, the time–temperature equivalence allows to aggregate the experimental data and to build a master curve for each ultimate property.

4.3. Fracture energy

The fracture energy J_c was computed from the experimental data using Eqs. (2) and (3). A FE analysis on a DENT specimen using the MSC.Marc software also allowed to compute the critical J integral. A comparison is shown in

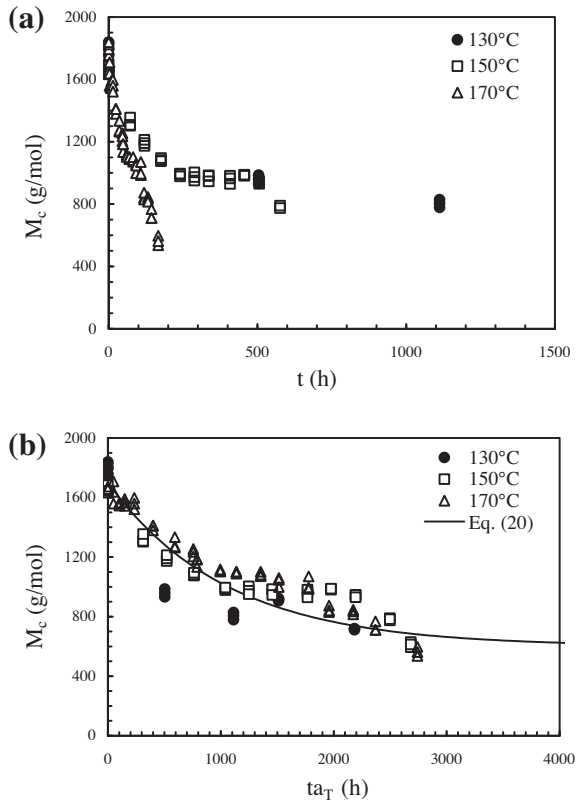

Fig. 3. Average molar mass as a function of: (a) the exposure time and (b) the reduced time, for three temperatures under study.

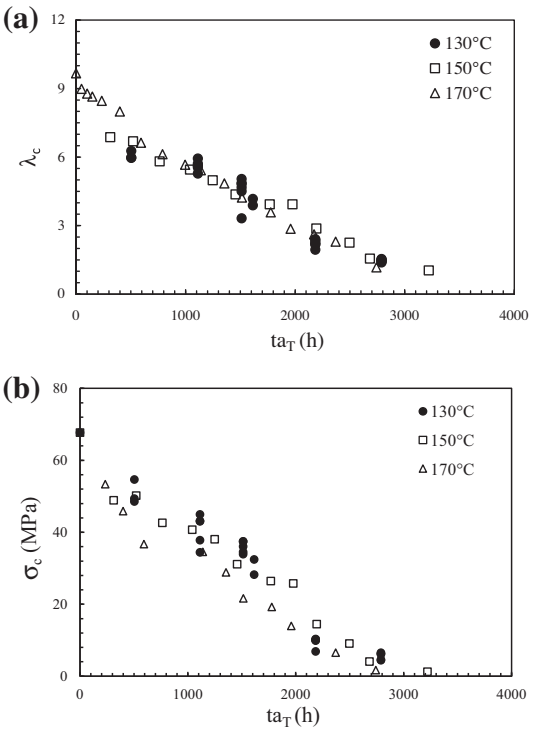

Fig. 4. Ultimate properties as a function of the reduced time: (a) failure stretch ratio and (b) failure stress.

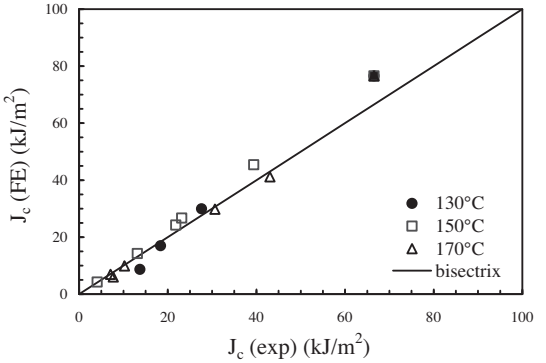

Fig. 5. Comparison between computed and measured fracture energies.

Fig. 5 where the FE results are plotted against the experimental data. All the dots lay around the bisectrix indicating a quite nice agreement.

The whole data are then reported in Fig. 6 as a function of the average molar mass square root and can be fitted by a linear law of the form:

$$J_c = \frac{A}{\sqrt{M_{c_0}}}\left(\sqrt{M_c} - \sqrt{M_{c_0}}\right) \tag{21}$$

where A and M_{c_0} are constants which values, given by a least square method, are 125 kJ/m^2 and 680 g/mol, respectively. This linear dependence on the average molar mass square root was reported for rubbers, but exclusively for the threshold fracture energy (Lake and Thomas, 1967).

4.4. Stress–strain relationship

Tensile tests allowed to obtain the evolution of the true stress as a function of the true strain. Fig. 7 shows an example of these relationships for an ageing temperature of 130 °C and for different exposure times. This figure clearly highlights that both the modulus and the hardening increase with respect to the ageing duration. Although only results for one temperature are given, the same trends were observed in the other studied temperatures.

The first-order Ogden SED function, given in Eq. (10), was used to describe the changes in the stress–strain relationship. This choice is reasonable and leads to a quite good description of our experimental results, as shown in Fig. 8 for particular examples.

The parameters μ and α of the Ogden model (Note that the suffix 1 is suppressed) were determined for each ageing condition. Fig. 9 shows the evolution of the shear modulus μ as a function of the average molar mass. Are also plotted the evolution of the theoretical modulus in the case of the phantom network for two crosslink functionality values. It is worth noting that the experimental data are bounded by the theoretical phantom network model.

The exponent α is then plotted as a function of the average molar mass in Fig. 10. This parameter decreases when increasing the average molar mass. Its value ranges

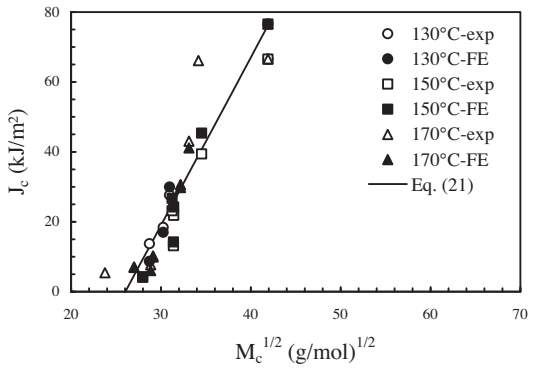

Fig. 6. Fracture energy as a function of the average molar mass square root.

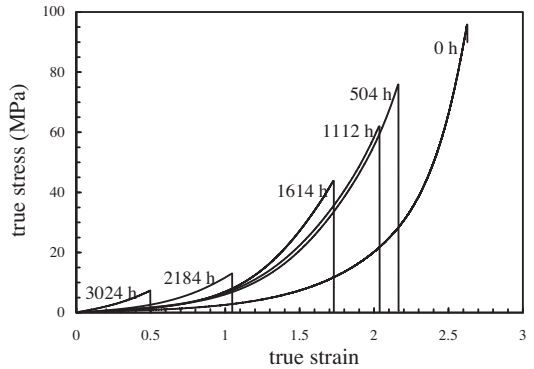

Fig. 7. Changes in the stress–strain relationship for an ageing temperature of 130 °C.

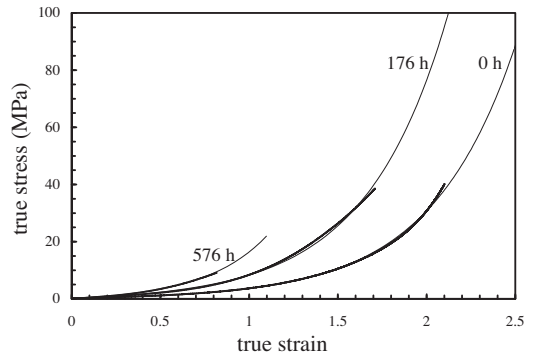

Fig. 8. Comparison between first-order Ogden model (dashed lines) and experiments (solid lines).

between 3 and 2, this latter value corresponding to a Neo-hookean model.

5. Prediction of the ultimate properties

In this section, we plan to build a prediction criterion by combining the intrinsic defect concept with the fracture mechanics approach. The main idea is that a material is never perfect and contains defects or heterogeneities (aggregates of reinforcement particles usually carbon black, voids, or defects induced during processing or pre-ageing, etc.). These pre-existing defects can act as stress concentrators when loading a specimen. The intrinsic defect approach is therefore used to predict the failure of smooth specimens. This approach was successfully used to predict the biaxial fracture of a Natural Rubber and a Styrene Butadiene Rubber (Naït-Abdelaziz et al., 2012). The prediction of the failure stretch ratios is achieved by using Eq. (4). In this equation, J_c is given by Eq. (21), a_{th} is the theoretical defect size and W is the SED. Knowing the critical value of J, and assuming that the failure of a specimen without crack is due to an intrinsic defect, it is possible to calculate the size of this defect which is assumed to be an intrinsic quantity of the material and thus equal to a constant. Moreover, the degradation of the macroscopic material behaviour is a direct consequence of the changes in the material microstructure. In this work, we assume that the dominant parameter that governs the mechanical properties, and is a pertinent indicator of the macromolecular network degradation, is the average molar mass of the elastically active chains M_c. So, capturing the evolution of this property with the exposure time would allow to predict the evolution of the macroscopic mechanical properties.

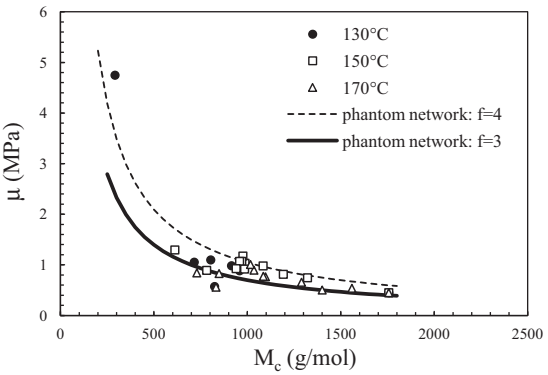

Fig. 9. Shear modulus μ as a function of the average molar mass.

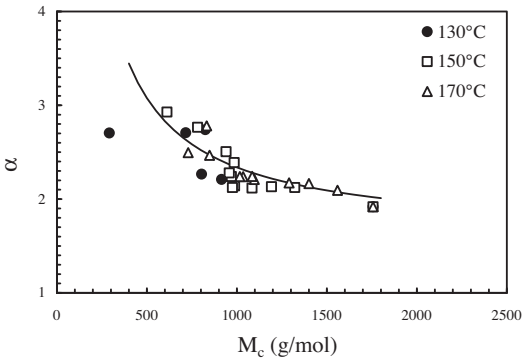

Fig. 10. Exponent α as a function of the average molar mass.

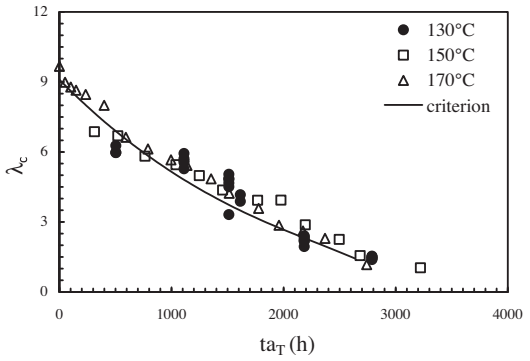

Fig. 11. Prediction of the failure stretch ratio as a function of the reduced time.

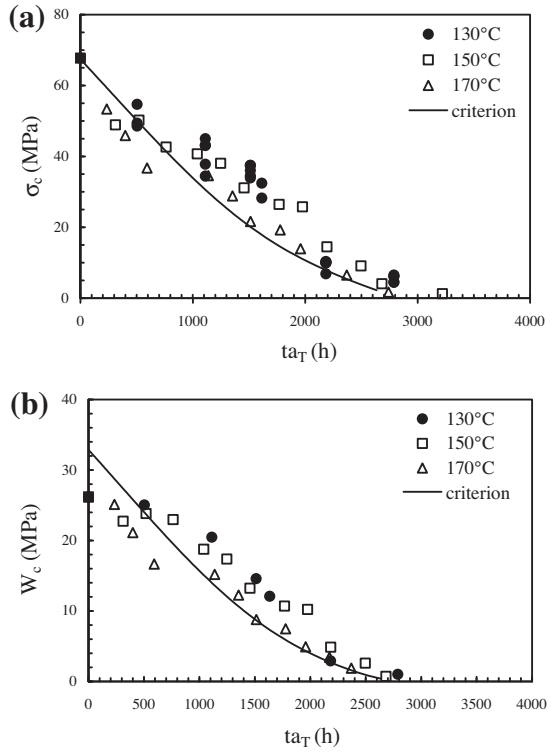

Fig. 12. Prediction of the failure stress (a) and the critical SED (b) as a function of the reduced time.

5.1. Determination of the intrinsic defect size

Considering the virgin material, the fracture energy at room temperature is first determined using a DENT specimen. For the DENT specimen (Fig. 1c), the fracture energy (equivalent to the J integral) could be written as:

$$J = T = 4kW_0a \tag{22}$$

Note that it is twice the value of the SENT specimen given in Eq. (2) because the specimen contains two cracks. In Eq. (22), W_0 is the SED of the virgin material, a is the crack length (5 mm in our case) and k is a decreasing function of the applied stretch ratio λ according to (Lake and Thomas, 1967):

$$k = \frac{\pi}{\sqrt{\lambda}} \tag{23}$$

By using Eq. (22), we have obtained a value of 66 kJ/m^2 for J_c. A FE analysis on the same specimen gives a critical J integral value of 70 kJ/m^2 which is in good agreement with the experimental value. Thus, the failure stretch ratio of a virgin smooth specimen being available, the theoretical defect size a_{th} can be computed using Eq. (4). The value we have obtained is 230 μm for J_c = 66 kJ/m^2. If we use the FE result of J_c (70 kJ/m^2), the value of a_{th} is 250 μm (radius of a circular defect in a tensile smooth specimen).

5.2. Prediction of the failure stretch ratio

As mentioned above, the degradation of the material properties is assumed to be strictly linked to the evolution of the average molar mass. The prediction of the failure stretch ratios is achieved by using Eq. (4). In this equation, J_c is given by Eq. (21), a_{th} is the virtual defect size already estimated and W is the SED. This SED can be calculated by using the Ogden formula given by Eq. (10) since the model parameters are directly related to the average molar mass M_c. To simplify the procedure, we assume, in what follows, a phantom network model which implies that the shear modulus is given by Eq. (13) with a crosslink functionality equal to 4. The exponent α is considered as a constant and equal to 2.

When the fracture occurs, Eq. (4) can therefore be rewritten as follows:

$$\frac{A}{\sqrt{M_{c_0}}}\left(\sqrt{M_c}-\sqrt{M_{c_0}}\right) = 2\lambda_{eq_c}^{\gamma} g(\lambda_{eq_c}) \times \frac{\rho RT}{2M_c}\left(1-\frac{2}{f}\right)\left(\lambda_c^2+\frac{2}{\lambda_c}-3\right)a_{th} \tag{24}$$

where $\lambda_{eq_c} = \sqrt{(\lambda_c^2 + 2\lambda_c^{-1})/3}$ in uniaxial tension and g is given by Eq. (6). The exponent γ is taken equal to 1. The suffix c denotes the critical value, i.e. that corresponding to the specimen fracture.

Since Eq. (24) is non-linear, it is solved numerically to estimate the failure stretch ratio λ_c for a given value of the average molar mass. Moreover, the average molar mass being linked to the reduced time by Eq. (20), it is therefore possible to plot the estimated failure stretch ratio as a function of the reduced time. The predicted evolution is compared to the experimental data in Fig. 11. A very nice agreement is obtained confirming that the intrinsic defect concept combined with the fracture mechanics can be used to derive a failure criterion accounting for the degradation due to ageing.

5.3. Prediction of the failure stress and the critical strain energy density

The Cauchy stress tensor components can be derived from the SED function W. In the principal directions, it is

given, for an incompressible material, by the following formula:

$$\sigma_i = \lambda_i \frac{\partial W}{\partial \lambda_i} + p \tag{25}$$

where p is the hydrostatic pressure determined by using the boundary conditions of the problem. For example, under uniaxial tension, only one component takes a non-zero value. In this case, the term p is determined using for example the condition $\sigma_2 = 0$. Using the SED function given by Eq. (15), the Cauchy stress under uniaxial tension is expressed as follows:

$$\sigma = \frac{\rho RT}{M_c}\left(1 - \frac{2}{f}\right)\left(\lambda^2 - \frac{1}{\lambda}\right) \tag{26}$$

The failure stress is obtained when the stretch ratio takes its critical value λ_c previously estimated. Using the same time–temperature equivalence derived from the average molar mass evolution, the failure stress can be plotted as a function of the reduced time as shown in Fig. 12a. The experimental data are in good agreement with the estimated stresses derived from the intrinsic defect criterion. Finally, as shown in Fig. 12b, we can also estimate the critical strain energy density by using Eq. (15) provided that λ is replaced by λ_c.

6. Conclusion

The objective of this study was to establish a failure criterion accounting for degradation due to ageing in the case of rubbers. First, from accelerated ageing tests, we have experimentally determined the changes in the ultimate mechanical properties such as the failure stretch ratios and stresses or the fracture energy in terms of critical J integral. Since degradation due to the thermal oxidation results in a competitive process of post-crosslinking versus chain scission, it is necessary to introduce microstructure features in the description of the material behaviour. The average molar mass of the elastically active chains (i.e. between crosslinks) was found to be a good indicator of degradation of the macromolecular network. Moreover, using the time–temperature equivalence combined with the Arrhenius model, we have shown that a master curve representing the evolution of the average molar mass as a function of a reduced time could be obtained. The activation energy was found in the same order of magnitude than that generally given in the literature. Using this activation energy and applying the same model, master curves were derived for the ultimate mechanical properties such as failure stretch ratios and stresses or critical strain energy density.

On the other hand, fracture mechanics tests on DENT specimens allowed to determine the fracture energy in terms of critical J integral which was found linearly dependent on the average molar mass square root. Finally, tensile tests allowed to derive the stress–strain relationship which can be fitted by using a first-order Ogden model. We have shown that, in a first approximation, the phantom network could be alternatively used to describe the material behaviour, provided that the functionality junction parameter is set to 4. Such a description allows to introduce the average molar mass as the main influent parameter on the mechanical response.

Combining the intrinsic defect concept with the fracture mechanics, we can therefore derive prediction of the ultimate properties. This approach requires as inputs, the average molar mass master curve, the evolution of the critical J integral versus the average molar mass and the intrinsic defect size. It also requires the stress–strain relationship which could be, as a first approximation, given by the phantom network theory. Finally, we have shown that the predicted values for all the ultimate properties are in good agreement with the experimental data.

Using such a method allows to predict time to failure for lower operating temperatures and makes therefore this tool very attractive when designing rubber components subjected to thermal oxidative environment.

Even the failure analysis was only based upon uniaxial tension and monotonic loading, it could be extended to any biaxial monotonic loading by using the approach we have developed in a previous paper (Naït-Abdelaziz et al., 2012). For non-monotonic loading paths, it will be necessary to account for the viscous effects. Such a modeling is actually in progress.

References

Ajalesh Balachandran, N., Kurian, P., Rani, J., 2012. Effect of aluminium hydroxide, chlorinated polyethylene, decabromo biphenyl oxide and expanded graphite on thermal, mechanical and sorption properties of oil-extended ethylene–propylene–diene terpolymer rubber. Mater. Des. 40, 80–89.

Arruda, E.M., Boyce, M.C., 1993. A three-dimensional constitutive model for the large stretch behavior of rubber elastic materials. J. Mech. Phys. Solids 41, 389–412.

Assink, R.A., Gillen, K.T., Sanderson, B., 2002. Monitoring the degradation of a thermally aged EPDM terpolymer by ^{1}H NMR relaxation measurements of solvent swelled samples. Polymer 43, 1349–1355.

Baldwin, F.P., Ver Strate, G., 1972. Polyolefin elastomers based on ethylene and propylene. Rubber Chem. Technol. 45, 709–881.

Braden, M., Gent, A.N., 1960. The attack of ozone on stretched rubber vulcanizates. II. Conditions for cut growth. J. Appl. Polym. Sci. 3, 100–106.

Bueche, F., 1959. The tensile strength of elastomers according to current theories. Rubber Chem. Technol. 32, 1269–1285.

Cherepanov, G.P., 1968. Cracks in solids. Int. J. Solids Struct. 4, 811–831.

Choi, I.S., Roland, C.M., 1996. Intrinsic defects and the failure properties of cis-1,4 polyisoprenes. Rubber Chem. Technol. 69, 591–599.

Clavreul, R., 1997. Evolution of ethylene propylene copolymers properties during ageing. Nucl. Instrum. Methods Phys. Res., Sect. B 131, 192–197.

Colin, X., Audouin, L., Verdu, J., 2007a. Kinetic modelling of the thermal oxidation of polyisoprene elastomers. Part III – oxidation induced changes of elastic properties. Polym. Degrad. Stab. 92, 906–914.

Colin, X., Audouin, L., Verdu, J., 2007b. Kinetic modelling of the thermal oxidation of polyisoprene elastomers. Part I – unvulcanized unstabilized polyisoprene. Polym. Degrad. Stab. 92, 886–897.

Colin, X., Audouin, L., Le Huy, M., Verdu, J., 2007c. Kinetic modelling of the thermal oxidation of polyisoprene elastomers. Part II – effect of sulfur vulcanization on mass changes and thickness distribution of oxidation products during thermal oxidation. Polym. Degrad. Stab. 92, 898–905.

Ferry, J.D., 1970. Viscoelastic properties of polymers. Br. Polym. J., New York: John Wiley & Sons, Ltd.

Gent, A.N., Lindley, P.B., Thomas, A.G., 1964. Cut growth and fatigue of rubbers. Part I: the relationship between cut growth and fatigue. J. Appl. Polym. Sci. 8, 455–466.

Gillen, K.T., Bernstein, R., Clough, R.L., Celina, M., 2006. Lifetime predictions for semi-crystalline cable insulation materials: I. Mechanical properties and oxygen consumption measurements on EPR materials. Polym. Degrad. Stab. 91, 2146–2156.

Greensmith, H.W., 1963. Rupture of rubbers. X. The change in stored energy on making a small cut in a test piece held in simple extension. J. Appl. Polym. Sci. 7, 993–1002.
Griffith, A.A., 1921. The phenomenon of rupture and flow in solids. Philos. Trans. R. Soc. J. Ser. A 221, 163–198.
Ha-Anh, T., Vu-Khanh, T., 2005. Prediction of mechanical properties of polychloroprene during thermo-oxidative aging. Polym. Testing 24, 775–780.
Hilborn, J., Ranaby, B., 1989. Photocrosslinking of EPDM elastomers. Photocrosslinkable compositions. Rubber Chem. Technol. 62, 592–608.
James, H.M., Guth, E., 1943. Theory of elastic properties of rubbers. J. Chem. Phys. 11, 455–481.
Lake, G.J., Thomas, A.G., 1967. The strength of highly elastic materials. Proc. R. Soc. Ser. A 300, 108–119.
Lindley, P.B., 1972. Energy for crack growth in model rubber components. J. Strain Anal. Eng. Des. 7, 132–140.
Marzocca, A.J., 2007. Evaluation of the polymer-solvent interaction parameter χ for the system cured styrene butadiene rubber and toluene. Eur. Polym. J. 43, 2682–2689.
Naït-Abdelaziz, M., Zaïri, F., Qu, Z., Hamdi, A., Aït Hocine, N., 2012. J integral as a fracture criterion of rubber-like materials using the intrinsic defect concept. Mech. Mater. 53, 80–90.
Ogden, R.W., 1984. Non linear elastic deformation. Ellis-Horwood Limited Publishers, England.
Rajeev, R.S., De, S.K., Bhowmick, A.K., John, B., 2003. Studies on thermal degradation of short melamine fibre reinforced EPDM, maleated EPDM and nitrile rubber composites. Polym. Degrad. Stab. 79, 449–463.
Rice, J.R., 1968. A path independent integral and the approximate analysis of strain concentration by notches and cracks. J. Appl. Mech. 35, 379–386.
Rivaton, A., Cambon, S., Gardette, J.L., 2005. Radiochemical ageing of EPDM elastomers. 3. Mechanism of radiooxidation. Nucl. Instrum. Methods Phys. Res., Sect. B 227, 357–368.
Rivlin, R.S., 1948. Large elastic deformations of isotropic materials. Philos. Trans. R. Soc. Ser. A 241, 459–525.
Rivlin, R.S., Thomas, A.G., 1953. Rupture of rubber. Part 1: characteristic energy for tearing. J. Polym. Sci. 10, 291–318.
Roland, C.M., Smith, C.R., 1985. Defect accumulation in rubber. Rubber Chem. Technol. 58, 806–814.
Tomer, N.S., Delor-Jestin, F., Singh, R.P., Lacoste, J., 2007. Cross-linking assessment after accelerated ageing of ethylene propylene diene monomer rubber. Polym. Degrad. Stab. 92, 457–463.
Trapper, P., Volokh, K.Y., 2008. Cracks in rubber. Int. J. Solids Struct. 45, 6034–6044.
Treloar, L.R.G., 1943. The elasticity of a network of long chain molecules. Trans. Faraday Soc. 39, 36–41.
Treloar, L.R.G., 1971. Viscoelastic properties of polymers. Br. Polym. J., London: John Wiley & Sons, Ltd.
Volokh, K.Y., 2013. Review of the energy limiters approach to modeling failure of rubber. Rubber Chem. Technol. 86, 470–487.
Williams, M.L., Landel, R.F., Ferry, J.D., 1955. The temperature dependence of relaxation mechanisms in amorphous polymers and other glass-forming liquids. J. Am. Chem. Soc. 77, 3701–3707.
Woo, C.S., Park, H.S., 2011. Useful lifetime prediction of rubber component. Eng. Fail. Anal. 18, 1645–1651.
Yeoh, O.H., 1990. Characterization of elastic properties of carbon black filled rubber vulcanizates. Rubber Chem. Technol. 63, 792–805.